Evaluating a Genesis Potential Index with Community Climate System Model Version 3 (CCSM3)

By: Kieran Bhatia

I. Introduction

To assess the impact of large-scale environmental conditions on tropical cyclone (TC) formation (hereafter referred to as TC genesis), scientists have used empirical methods to develop several "genesis parameters" or "genesis indices". These parameters are mathematical expressions that link observable meteorological variables known to affect TC genesis with a likelihood that a TC will develop. Most indexes include dynamical and thermodynamical parameters such as relative humidity, sea surface temperature, saturation deficit, wind shear, and vorticity. Each of these variables can emerge as the dominant term in the genesis parameter calculation depending on the time of the year and area of the Earth. Gray (1979) developed the first such index, and his work demonstrated that a genesis parameter can reproduce the seasonal cycle and spatial variability commonly observed with TCs. Since then, there have been many other attempts at formulating successful genesis parameters (e.g., Emanuel and Nolan 2004; Emanuel 2010; Tippett et al. 2011); there are tremendous ramifications for an accurate genesis potential index. One of society's most pressing challenges is determining how TCs are affected by climate change. Several studies have evaluated the past performance of the genesis parameters at forecasting TC frequency to determine if the parameters have the potential to project future TC genesis events (Zhang et al. 2010; Camargo et al 2007). Most state-of-the-art Global Climate Change Models (GCMS) can provide fairly accurate reproduction of large scale features for the past and present climate, so effective genesis parameters could theoretically diagnose climate change's impact on TC frequency.

These genesis indices are also useful because they highlight the relative importance of different environmental factors for TC genesis. In 2007, Camargo et al.

not only assessed the role of each variable in the genesis potential index (GPI) developed my Emanuel and Nolan (2004) but also tested the GPI's ability to represent the climatological patterns of TCs. Camargo et al. began their GPI evaluation by using monthly NCEP Reanalysis data from 1950 to 2005 to calculate global GPI values and compared these values to the location of post 1970s genesis events recorded by the NOAA National Hurricane Center and U.S. Navy's Joint Typhoon Warning Center. The study showed the global distribution and seasonal variation in the GPI agreed well with the actual TC genesis locations. Still, Camargo et al. alluded to the fact they completed a slight adjustment of Emanuel and Nolan's GPI to better fit the genesis events to observational data (important to note for comparison to this work's figures). Another focus of the Camargo et al. study was monitoring the ability of the GPI to capture the effects of the El Niño-Southern Oscillation (ENSO) on global TC genesis frequencies. During ENSO, the global climate system is significantly changed which has obvious implications for TC genesis. In the eastern and central equatorial Pacific Ocean basin, sea surface temperatures are anomalously high and vertical shear is lower than normal so conditions are more favorable for TC activity (Univ. of Rhode Island). At the same time, ENSO suppresses TC genesis in the Atlantic basin largely due to higher vertical shear in the TC main development region (10^oN - 20° N, 20° W- 85° W). La Niña typically leads to reversed conditions in each of these basins. Therefore, Camargo et al. (2007) listed ENSO as the "largest single predictable factor influencing genesis in some basins" so the legitimacy in the GPI hinges on its ability to capture these ENSO trends.

The goal of this study is to follow a similar method described in Camargo et al. (2007) to evaluate the GPI's ability to capture the seasonal and interannual variability of

genesis. A 100 year control run from the CCSM3 provided the necessary environmental variables to calculate the GPI. First, several tests were conducted to ensure the model was demonstrating the correct seasonal variability of large scale parameters like sea surface temperature, zonal wind, meridional wind, and relative vorticity. Then, the GPI was calculated and its annual cycle was verified with comparisons to other notable results (Tippet et al. 2011; Zhang 2010). Finally, a technique similar to the one used by Camargo et al. was used to define El Niño, La Niña, and ENSO neutral years. CCSM3's ENSO signal is described and compared to other studies. CCSM3 is assumed to be relatively accurate for large-scale variables; the improved model physics along with the T85 grid for the atmosphere and land and a grid with approximately 1° resolution for the ocean and sea ice is sufficient for this study's analysis (Collins et al. 2006). The model accuracy has important implications for the assessment of the GPI, and the consequences of CCSM3's possible flaws on the GPI results are also considered.

II. Calculation of the GPI for the CCSM3

Emanuel and Nolan (2004) constructed their GPI based largely on Gray's (1978) seminal paper with one notable exception, their treatment of the environment's thermodynamic control on TC genesis. Instead of using just sea surface temperature, the GPI incorporates potential intensity, which depends more on the air-sea thermodynamic imbalance. The definition of the GPI used is as follows:

$$\text{GPI} = |10^5 \eta|^{3/2} \left(\frac{\mathcal{H}}{50}\right)^3 \left(\frac{V_{\text{pot}}}{70}\right)^3 (1 + 0.1 V_{\text{shear}})^{-2} \tag{1}$$

where η is the absolute vorticity at 850 hPa (in s^-1), H is the relative humidity at 600 hPa in percent, V_{pot} is the potential intensity (in m/s), and V_{shear} is the magnitude of the

vertical wind shear between 850 hPa and 200 hPa (in m/s). The index represents a rate

per unit time per unit area, but for the GPI magnitude and dimensions to represent a

realistic TC frequency, an appropriate coefficient must be introduced (comparing

magnitudes spatially is sufficient for this study). Each of the GPI terms is analyzed to

ensure they displayed a realistic seasonal cycle, and Figure 1 shows the 100-year

monthly mean from the CCSM3 run of the maximum potential intensity (MPI) during

February and September, within the peak of the tropical cyclone season in the Southern

and Northern Hemisphere, respectively. Figure 1 accurately captures the seasonal

variation of MPI. The potential intensity (VMAX) displays its highest values in the

Southern Hemisphere during February, with the appropriate maximum in the southern

Indian Ocean and northeast Australia (Zhang et al. 2010). Additionally, the September

VMAX distribution is also realistic with its highest values in the northern hemisphere,

specifically in locations like the western Pacific Ocean basin and Atlantic Ocean main

development region.

   After deeming all of the constituents of the GPI as reasonable, mean GPI is

calculated for each month, and the annual cycle is evaluated. Figure 2 shows the

climatological mean values of the CCSM3 GPI in February and September. This figure

was compared to Fig. 3 in Tippett et al. (2011) and Fig. 1 in Camargo et al. (2007).

Again, the GPI shows a reasonable annual cycle and the maximums in GPI occur in

areas similar to the two mentioned papers. The only notable difference shows up in the

Caribbean Sea where it appears the CCSM3 GPI is slightly less than what is typical for

September. It is possible that the continental mask developed for this study's figures

might hide some of these high GPI values.

III. GPI and ENSO

ENSO has a major influence on TC genesis frequency in all the ocean basins. The atmospheric and oceanic variables that are responsible for changing TC genesis frequencies during ENSO events are the main constituents of the GPI calculation. To assess ENSO's influence on CCSM3's GPI, the GPI's monthly anomalies (subtracted from each month's long-term mean) were computed for the 100-year period. From these anomalies, three-month running means were computed. The three-month running means as well as the Niño-3.4 index served as a basis for defining El Niño and La Niña events. The years with the twenty-five highest (lowest) Niño-3.4 values for the August to October (ASO) running mean were defined as El Niño (La Niña) years for the Northern Hemisphere. The twenty-five highest (lowest) Niño-3.4 values for the January to March (JFM) running mean were defined as El Niño (La Niña) years for the Southern Hemisphere. Focusing on the ASO La Niña and El Niño results (Fig .3), the GPI anomalies have a maximum in eastern and central Pacific Ocean just above the equator. The change in sign from positive to negative GPI in this region is not seen in nature.

Also, the normal anomalies in different parts of the world are not visible due to the extreme GPI anomalies in this Pacific region. On the other hand, the opposite signs for the anomalies for La Niña and El Niño in the western Pacific Ocean are well-grounded. However, the expected negative GPI anomaly in the Atlantic basin is not visible in Figure 3. By zooming into the main genesis region in the Atlantic Ocean and adjusting the color bar accordingly, the expected anomalies are visible. Their magnitude

is overshadowed by the eastern and central Pacific Ocean anomalies. Figure 4 shows El Niño - La Niña GPI in the Atlantic Ocean. The negative values in the main development region are appropriate and confirm that El Niño lowers GPI in the Atlantic basin compared to La Niña in the CCSM3 model. Figure 5 justifies the lower GPI in the Atlantic Ocean during El Niño years by depicting the increased shear in the Atlantic main development region. Also, equation 1 confirms that higher shear values lead to lower GPI.

IV. Conclusion

The genesis parameter is a useful tool that translates large-scale variables into a prediction of tropical cyclone activity. Numerous studies have verified the accuracy of genesis parameters with observational data and climate models. Nolan (2011) compared some of these parameters, and they often show comparable results because GPI equations are all composed of similar variables. CCSM3's GPI captures the seasonal cycle and annual variability of global TC activity. Future work involves evaluating Emanuel's (2010) new genesis parameter, which is dimensionally correct and is demonstrated to fit observational data better. Emanuel's new GPI has been coded up by the author of this work, and figures using the CCSM3 are available upon request.

V. References

Camargo, S.J., K.A. Emanuel and A.H. Sobel, 2007. Use of a genesis potential index to diagnose ENSO effects on tropical cyclone genesis. Journal of Climate, 20, 4819-4834.

Collins, W. D., and Coauthors, 2006a: The Community Climate System Model version 3 (CCSM3). *J. Climate,* **19,** 2122–2143.

Emanuel, K. A., and D. S. Nolan, 2004: Tropical cyclone activity and global climate preprints, 26th Conf. on Hurricanes and Tropical Meteorology, Miami, FL, Amer. Meteor. Soc., 240–241.

Emanuel, K. A., 2010: Tropical Cyclone Activity Downscaled from NOAA-CIRES Reanalysis, 1908-1958, J. Adv. Model. Earth Syst., Vol. 2, Art. #1, 12 pp., doi:10.3894/JAMES.2010.2.1 Published 27 Jan. '10.

Gray, W. M., 1979: Hurricanes: Their formation, structure and likely role in the tropical circulation. Meteorology over the Tropical Oceans, Royal Meteorological Society, 155–218.

Nolan, D. S., and Michael G. McGauley, 2011: Tropical cyclogenesis in wind shear: Climatological relationships and physical processes. To appear in Cyclones: Formation, Triggers, and Control. Kazuyoshi Ooouchi and Hironori Fudeyasu, eds., Nova Science Publishers, Happauge, New York.

Tippett, M.K., S.J. Camargo, and A.H. Sobel, 2011. A Poisson regression index for tropical cyclone genesis and the role of large-scale vorticity in genesis. Journal of Climate, 24, 2335-2357, doi: 10.1175/2010JCLI3811.1.

University of Rhode Island. Hurricanes: Science and Society website.

Zhang, Y. et al. Changes in the Tropical Cyclone Genesis Potential Index over the Western North Pacific in the SRES A2 Scenario. Advances In Atmospheric Sciences, VOL. 27, NO. 6, 2010, 1246–1258.
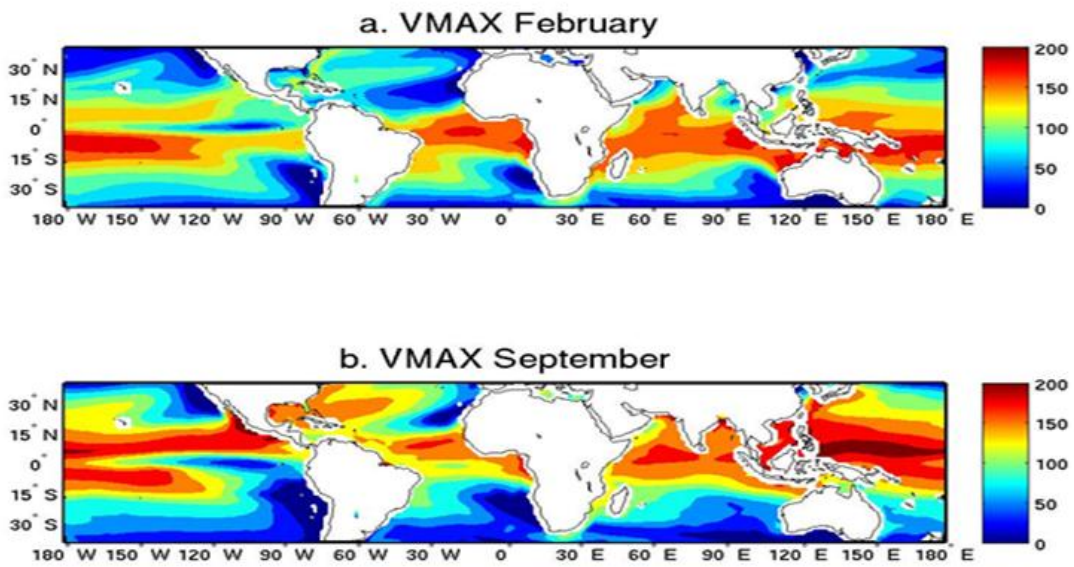
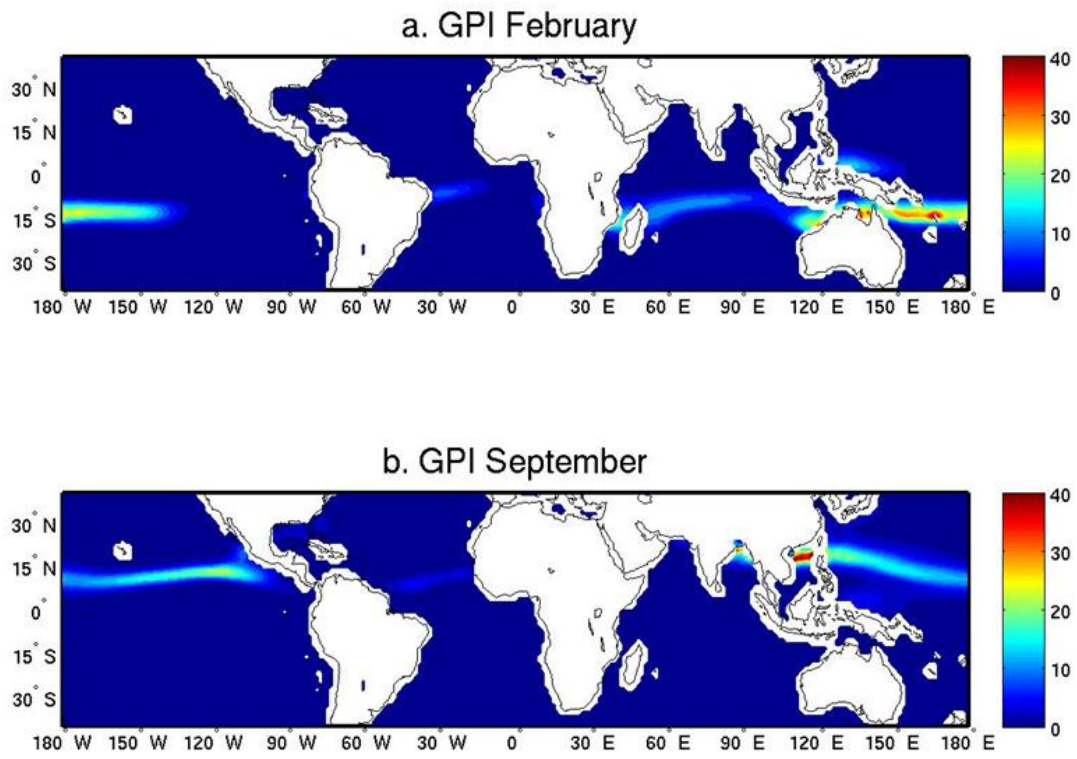Fig. 1. 100-year maximum potential intensity (m/s) mean at each grid point in a. February and b. September.

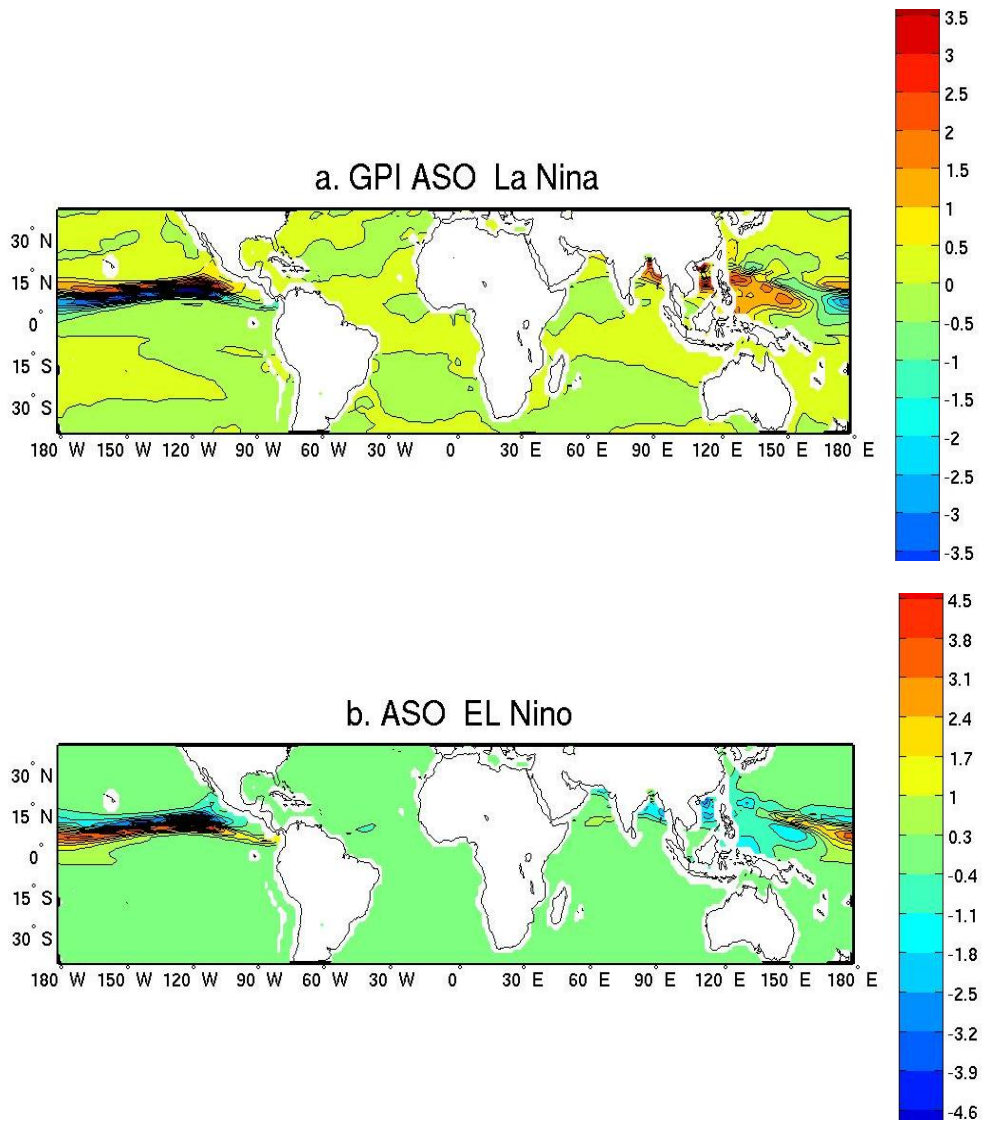Fig. 2. GPI 100-year mean values in a. February and b. September.

Fig. 3. GPI anomalies in ASO for a. La Niña and b. El Niño years compared to the 100-year mean.
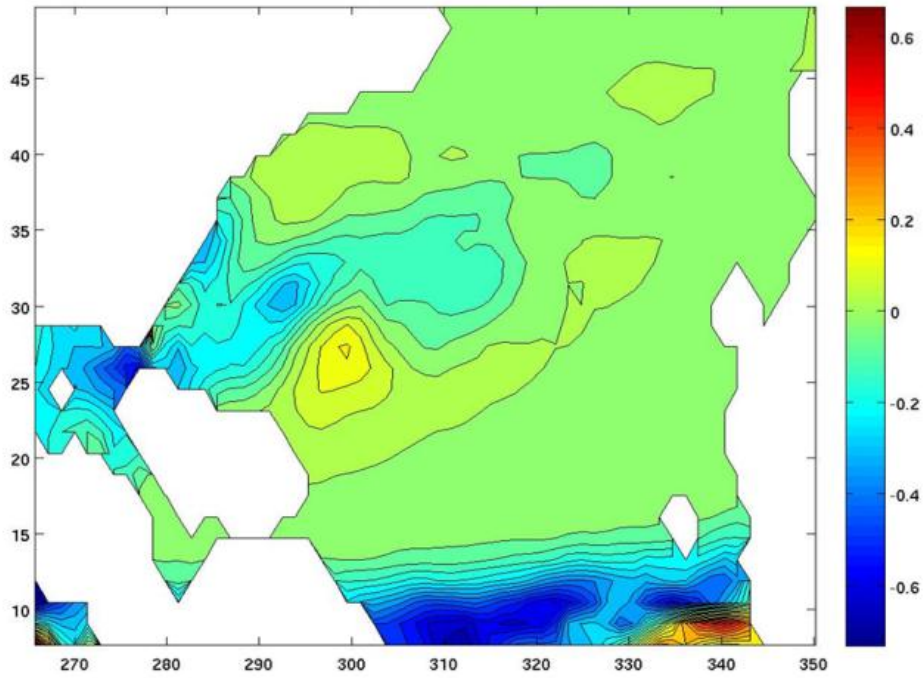
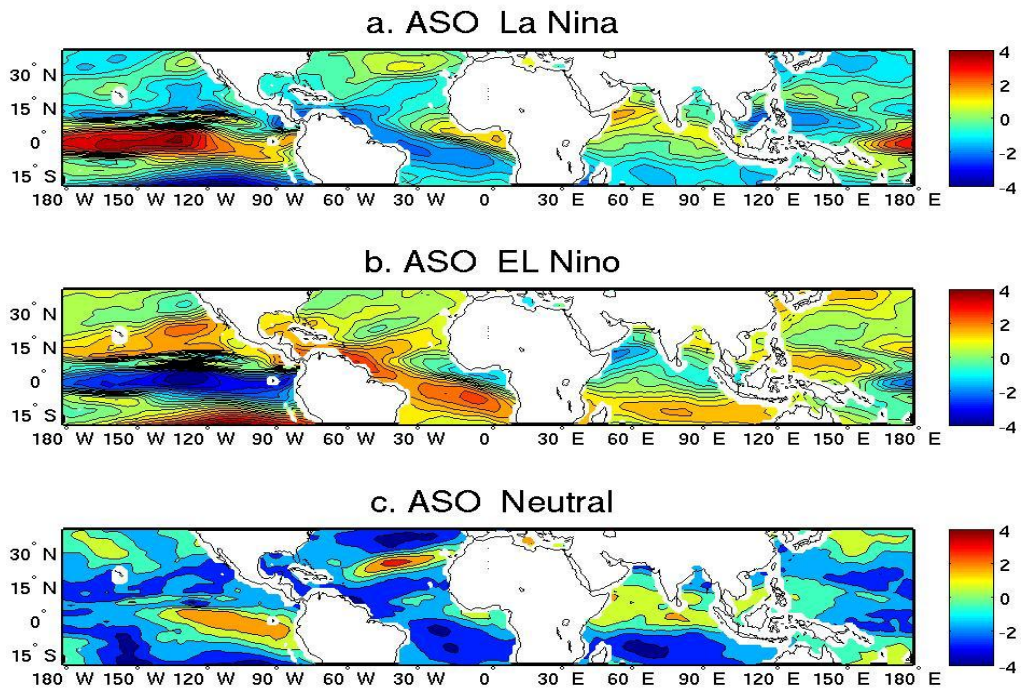Fig.4. GPI anomaly (El Niño –La Niña) in ASO for Atlantic Ocean Basin.

Fig. 5. Shear anomalies (m/s) in a. ASO La Niña years b. ASO El Niño years c. ASO Neutral Years compared to 100-year mean.